environmental microbiology

Environmental Microbiology (2019) **00**(00), 00–00 doi:10.1111/1462-2920.14836

Acclimation to low ultraviolet-B radiation increases photosystem I abundance and cyclic electron transfer with enhanced photosynthesis and growth in the cyanobacterium *Nostoc sphaeroides*

Zhen Chen,[1] Hai-Bo Jiang,[1] Kunshan Gao[2] and Bao-Sheng Qiu[1*]

[1]*School of Life Sciences, Hubei Key Laboratory of Genetic Regulation and Integrative Biology, Central China Normal University, Wuhan, Hubei, 430079, People's Republic of China.*

[2]*State Key Laboratory of Marine Environmental Science, Xiamen University, Xiamen, Fujian, 361005, People's Republic of China.*

Summary

Ultraviolet-B radiation is known to harm most photosynthetic organisms with the exception of several studies of photosynthetic eukaryotes in which UV-B showed positive effects. In this study, we investigated the effect of acclimation to low UV-B radiation on growth and photosynthesis of the cyanobacterium *Nostoc sphaeroides*. Exposure to 0.08 W m^{-2} UV-B plus low visible light for 14 d significantly increased the growth rate and biomass production by 16% and 30%, respectively, compared with those under visible light alone. The UV-B acclimated cells showed an approximately 50% increase in photosynthetic efficiency (α) and photosynthetic capacity (P_{max}), a higher PSI/PSII fluorescence ratio, an increase in PSI content and consequently enhanced cyclic electron flow, relative to those of non-acclimated cells. Both the primary quinone-type acceptor and plastoquinone pool re-oxidation were up-regulated in the UV-B acclimated cells. In parallel, the UV-B acclimated colonies maintained a higher rate of D1 protein synthesis following exposure to elevated intensity of UV-B or visible light, thus functionally mitigating photoinhibition. The present data provide novel insight into photosynthetic acclimation to low UV-B radiation and suggest that UV-B may act as a positive ecological factor for the productivity of some photosynthetic prokaryotes, especially during twilight periods or in shaded environments.

Received 28 May, 2019; accepted 18 October, 2019. *For correspondence. E-mail bsqiu@mail.ccnu.edu.cn; Tel. +86 27 67862470.

Introduction

The depletion of the stratospheric ozone layer since 1970s, mainly because of the release of anthropogenic atmospheric pollutants such as chlorofluorocarbons, has resulted in an increase in solar ultraviolet-B radiation (UV-B; 280–315 nm) that reaches the Earth's surface (Kerr and McElroy 1993; Bais et al. 2015). In most regions of the world, UV-B accounts for less than 1% of incident solar radiation, but its harm to aquatic and terrestrial organisms is much greater than that of UV-A (315–400 nm) in terms of biologically weighted impacts (Gao et al. 2007; Häder et al. 2015; Robson et al. 2019; Williamson et al. 2019). Irradiance with UV-B exerts detrimental effects on various photosynthetic organisms and different ecosystems (Kataria et al. 2014; Häder et al. 2015). It is extensively reported that enhanced UV-B has the potential to damage DNA, RNA, lipid, and protein directly or indirectly via the formation of reactive oxygen species, and consequently impairs cellular physiological and biochemical processes, such as development, motility, pigmentation, and enzyme of carbon and nitrogen fixation, resulting in the inhibition of growth in the natural environment (Takahashi et al. 2010; Rastogi et al. 2014; Häder et al. 2015; Cai et al. 2017). The negative effects of UV-B are offset by a number of defence strategies. These include the production of UV-absorbing sunscreen compounds, for example, flavonoids and other phenolic metabolites that accumulate in the epidermal layers of *Arabidopsis* (Li et al. 1993). Other defensive processes, such as efficient DNA repair mechanisms (Chen et al. 1994) and enhancement of antioxidant enzyme activities (Kataria et al. 2007), can repair UV damage and ameliorate oxidative stress.

However, the effect of UV-B is largely dependent on UV-B intensity and duration of irradiation, other environmental factors, and species (Häder et al. 2015; Williamson et al. 2019). The ambient intensity of UV-B in

solar radiation is variable and strongly affected by time of day, season, latitude, altitude, water depth, and meteorological factors (Hargreaves 2003; Paul and Gwynn-Jones 2003; Bais et al. 2015). Responses to UV-B exposure differ among organisms. Few studies have reported positive effects of UV-B on photosynthetic organisms. For example, UV-B acclimation in *Lactuca sativa* during early development (10 KJ m^{-2} d^{-1} UV-B, 23 d) leads to enhanced photoprotection and photosynthetic rate, and subsequently results in increased crop yield and improved resistance to other stresses, although the mechanisms underpinning the beneficial effects remain elusive (Wargent et al. 2011; Wargent et al. 2015). In addition, some researchers have observed that low or non-damaging intensities of UV-B can function as a key environmental signal and exert numerous regulatory effects (Jenkins 2009). It has been reported that UV-B can initiate photoreceptor UVR8-mediated UV-protective responses in Arabidopsis (*Arabidopsis thaliana*) (Brown et al. 2005; Jenkins 2009; Rizzini et al. 2011) and the photoprotective regulation of photosynthetic machinery in the green alga *Chlamydomonas reinhardtii* (Allorent et al. 2016). The majority of studies that have reported deleterious effects applied relatively high UV-B doses and emphasized the damage induced by UV-B irradiance. Thus, the ecophysiological significance of low-dose UV-B that reflects the UV-B intensity in ambient and future environments has been largely ignored. With the gradual recovery of the ozone layer as a result of implementation of the Montreal Protocol (Bais et al. 2015; Chipperfield et al. 2017), the UV-B dosage reaching the surface of the Earth will decline and the ecophysiological significance of low UV-B radiation should receive greater attention.

Cyanobacteria are the most ancient group of photosynthetic prokaryotes and contribute to about 25% of the total marine primary productivity (Flombaum et al. 2013). Cyanobacteria have a cosmopolitan distribution ranging from hot springs to the Arctic and Antarctic regions. They are believed to have originated in the Precambrian supereon in a period when the ozone shield was absent (Shih 2015). Cyanobacteria have evolved versatile tolerance and adaptation mechanisms against high fluxes of UV radiation, including avoidance, the scavenging of reactive oxygen species by enzymatic/nonenzymatic antioxidant molecules, the synthesis of UV-absorbing/screening compounds such as mycosporine-like amino acids (MAAs), the repair of UV-induced DNA damage, and protein resynthesis (Singh et al. 2010; Rastogi et al. 2014; Shang et al. 2019). The effects of the gradually decreasing intensity of ambient UV-B on cyanobacteria and their primary production require investigation. New knowledge may provide a novel opportunity to reevaluate primary productivity estimation associated with UV-B radiation in the future. Although many previous studies have reported on the damage of UV-B on photosynthesis, especially the oxygen-evolving complex, of cyanobacteria (Takahashi et al. 2010; Jiang and Qiu 2011), the majority of these studies employed a relatively high dose of UV-B, and thus the conclusion exaggerates the negative effects of UV-B damage, especially in the future under gradual recovery of ambient UV-B intensity. To date, positive effects of UV-B on the photosynthesis of cyanobacteria have not been reported.

Nostoc sphaeroides Kützing is a colony-forming and nitrogen-fixing cyanobacterium distributed on the sediment surface in the rice-field ecosystem (Qiu et al. 2002). In its habitat, light reaching *N. sphaeroides* colony is usually low because of a rapid decrease in light penetration resulted from the canopy of rice or weed, floating macrophyte, and plankton. Furthermore, *N. sphaeroides* forms spherical colonies reaching 0.5–2 cm diameter, and the inner cells are exposed to low solar radiation because of self-shading (Gao and Ai 2004). Thus, this species is a typical low-light adapted cyanobacterium in the nature environment. In the present study, we investigated the effects of low-dose UV-B on its growth and photosynthetic performance under low visible light, aiming to gain insight into the ecophysiological significance of low-dose UV-B.

Results

Low UV-B radiation promoted growth rate and biomass production of N. sphaeroides

Stages of spherical microcolony formation in *N. sphaeroides* are shown in Fig. 1. The hormogonium (Fig. 1A and B) first developed a sheath and became a vegetative filament with a visible heterocyst after 1 day of cultivation (Fig. 1C and D). When cell division started within the sheath, an aggregated cell mass was formed and expanded into pellicled colonies (Fig. 1E–H), and finally into spherical colonies after 6 days (Fig. 1I–L). The spherical microcolony formation was not influenced by low UV-B radiation, although the sheath around multiple filaments became thicker in UV-B-treated samples compared with that of the control within the first 6 days.

Growth of *N. sphaeroides* in response to low UV-B radiation plus low PAR is indicated in Fig. 2. To simulate low light niches, we exposed cultures to 4.35 W m^{-2} visible light and observed that *N. sphaeroides* was capable of rapid growth. Notably, when exposed to supplementary low UV-B radiation (0.08 W m^{-2}), the specific growth rate significantly increased by 16% (Fig. 2A and B) (*t*-test, $P < 0.05$). We further observed that dry biomass was significantly increased by 30% after 14 d exposure to UV-B plus PAR (*t*-test, $P < 0.05$), compared with that of the control (Fig. 2C). The content of MAAs in UV-B-treated

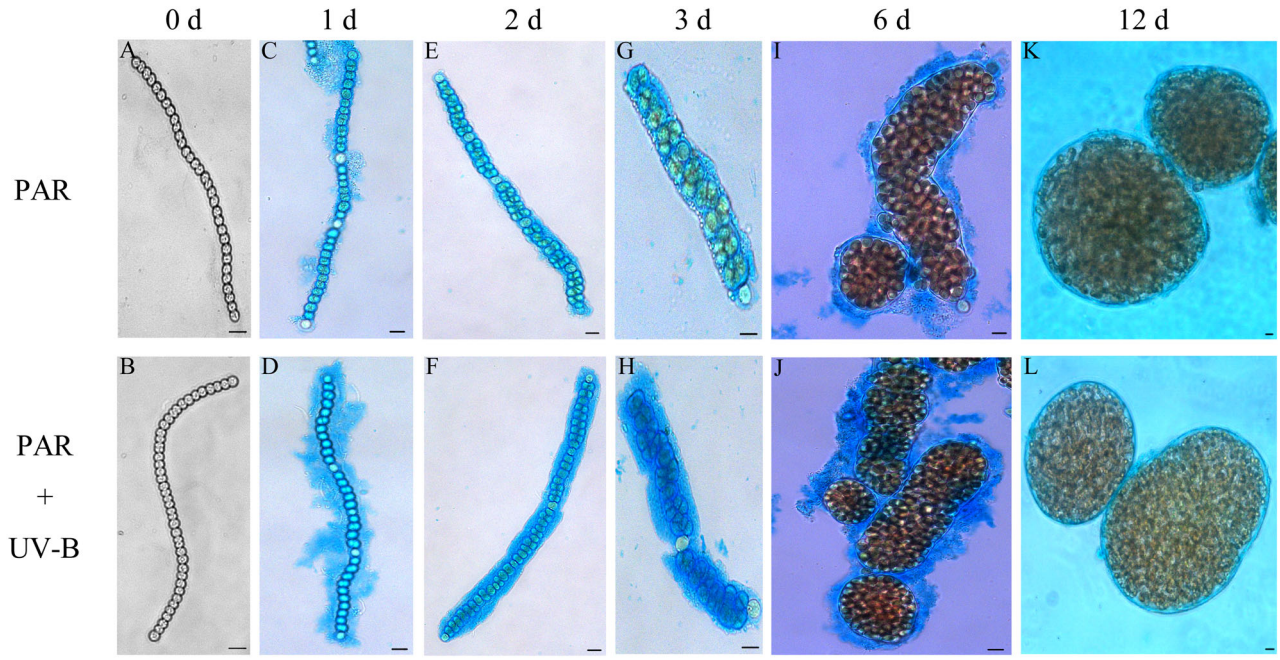

Fig. 1. Effects of UV-B radiation on spherical microcolony formation of *Nostoc sphaeroides*. Developmental stages of *N. sphaeroides*.
A, B. hormogonium.
C, D. filaments.
E–H. pellicled colonies.
I–L. spherical colonies.
Magnification of A–J: ×400. The colonies were stained with Alcian blue. Scale bar: 10 μm.

cells increased rapidly within 4 days, reaching 1.6 times that of the control, then gradually decreased to about 1.3 times that of the control, and thereafter remained stable during the exposure to low UV-B radiation (Fig. 2D).

PSI/PSII ratio of N. sphaeroides *increased after 8 days exposure to low UV-B radiation*

The PSI/PSII fluorescence ratio represents the amount of energy reaching the centres and is related to photosystem stoichiometry in cyanobacteria (Murakami 1997). The PSI/PSII fluorescence ratio (F_{725}/F_{685}) from the 77 K fluorescence emission spectra was detected in *N. sphaeroides* during exposure to PAR or PAR plus UV-B for 14 days (Figs. 2E and 3A). It exhibited no significant change in UV-B-treated cells compared with that of non-treated cells within 8 days, but then increased significantly and exceeded the control PSI/PSII fluorescence ratio during continued exposure to low UV-B radiation (Fig. 2E). After normalization of the PSII peak at 685 nm, the PSI/PSII fluorescence ratio in samples acclimated after 12 days exposure to UV-B increased by 33% compared with that of the control (*t*-test, $P < 0.05$) (Fig. 3A). The increase in the PSI/PSII fluorescence ratio might result from a decrease in PSII content or an increase in PSI content. To determine the nature of the enhanced PSI/PSII fluorescence ratio, we carried out immunoblots using antibodies of the PSII core subunits (anti-D1 and anti-CP47 antibody) and PSI core subunits (anti-PsaA/B and anti-PsaC antibody) for the control and UV-B acclimated colonies. No distinct changes in D1 and CP47 contents were observed, but the contents of PsaA/B and PsaC markedly increased in the UV-B acclimated samples (Fig. 3B). These results indicated that the PSII content was similar in the control and UV-B acclimated colonies, but PSI content increased after 12 days exposure to low UV-B radiation.

Cyclic electron flow around PSI was up-regulated in UV-B acclimated N. sphaeroides

The PSI photochemical activity was assayed in *N. sphaeroides* after 12 days exposure to PAR or PAR plus UV-B (Fig. 3C–E). We measured the *in vivo* oxidizing photochemical activity of PSI represented by changes in P_{700} absorbance in the presence of DCMU. The maximal P_{700} signal increased by 33% compared with that of the control (Fig. 3C), which indicated that low UV-B radiation induced higher oxidizing photochemical activity of PSI.

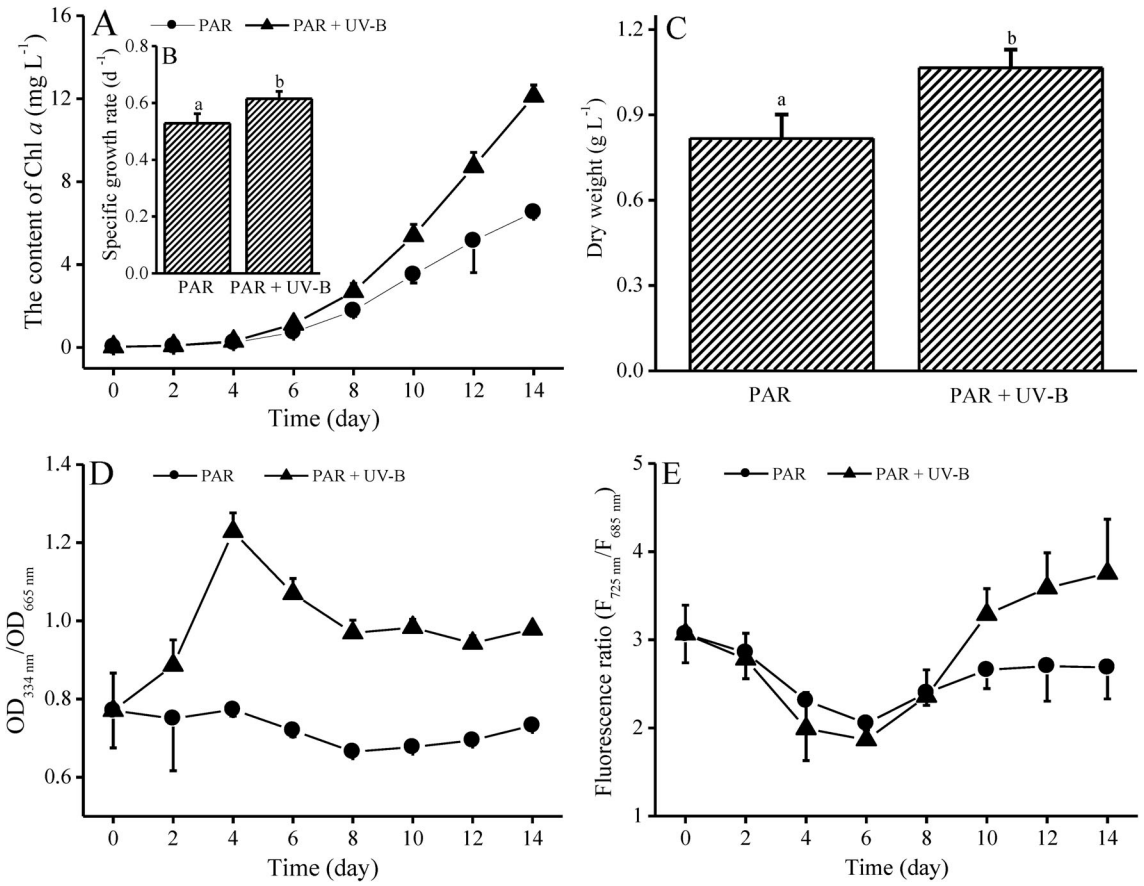

Fig. 2. Effects of UV-B radiation on growth, MAAs content, and PSI/PSII fluorescence ratio of *Nostoc sphaeroides*.
A, B. Growth based on chlorophyll *a* (Chl *a*) content during 14 d exposure to photosynthetically active radiation (PAR) or PAR plus UV-B radiation.
C. Dry weight after 14 d exposure to UV-B.
D. Content of UV-absorbing mycosporine-like amino acids (MAAs) based on the ratio of absorption at 334 nm (MAAs) to 665 nm (Chl *a*).
E. The PSI/PSII fluorescence ratio (F_{725nm}/F_{685nm}) determined from the 77 K fluorescence emission spectra. Bars with different superscript letters for the same parameter are significantly different (*t*-test, $P < 0.05$). Data are means ± SD (n = 5–6 for A, B, D & E; n = 15–16 for C).

We also monitored the P_{700}^+ reduction kinetics in *N. sphaeroides* (Fig. 3D and E). The P_{700}^+ reduction rate constants (s^{-1}) were determined from the calculated electron transfer rate (Table 1). The P_{700}^+ reduction kinetics in the absence of inhibitors is a measure of the total net electron flow (linear + cyclic) through PSI. No significant difference between the control and UV-B acclimated samples was observed in the absence of inhibitors (Fig. 3D and E; Table 1). To determine cyclic electron flow of the samples, 20 μM DCMU was added prior to P_{700}^+ reduction measurement to block the photosynthetic linear electron transfer pathway. The cyclic electron transfer rate of 2.21 ± 0.23 s^{-1} in UV-B acclimated cells was nearly two-fold that of non-acclimated cells (0.99 ± 0.13 s^{-1}), and the contribution of cyclic electron flow in UV-B acclimated cells (10.8%) was two times that in non-acclimated cells (5.5%) (Fig. 3D and E; Table 1). Methyl viologen accepts electrons from the acceptor side of PSI (Yu et al. 1993) and can block the cyclic electron flow around PSI. The monitored P_{700}^+ reduction in the presence of both DCMU and MV represents the electrons flowing through PSI that are derived from the respiratory electron transport chain. In the presence of both DCMU and MV, the P_{700}^+ reduction rate was slightly higher under UV-B radiation (Fig. 3D and E; Table 1), but no significant difference in the contribution of the electron influx for PSI reduction was observed between the control and UV-B acclimated cells. These results showed that cyclic electron flow was up-regulated under low UV-B radiation in *N. sphaeroides*.

Q_A and PQ pool reoxidation were more rapid in UV-B acclimated N. sphaeroides

The effects of low UV-B radiation on PSII function of *N. sphaeroides* are summarized in Table 2. The PSII activity ($H_2O \rightarrow p$-BQ) and maximal quantum yield of PSII photochemistry (F_v/F_m) were not significantly affected by

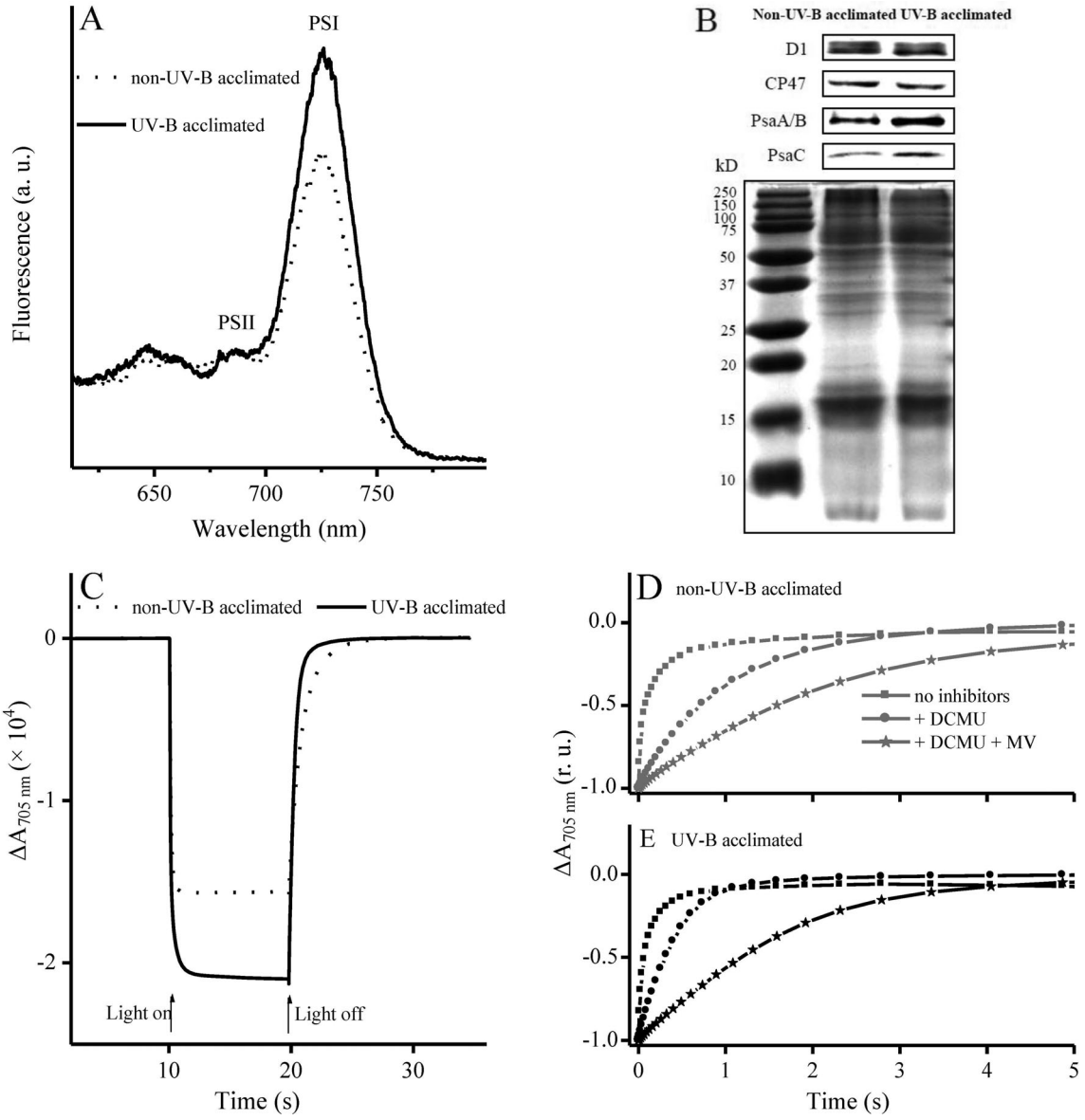

Fig. 3. Effects of 12 days exposure to UV-B radiation on photosystem I (PSI) function of *Nostoc sphaeroides*.
A. 77 K fluorescence emission spectra. The excitation wavelength was 435 nm, and spectra were normalized to photosystem II (PSII) absorption at 685 nm.
B. Core proteins of PSII (D1 and CP47) and PSI (PsaA/B and PsaC). After exposure to photosynthetically active radiation (PAR) or PAR plus UV-B radiation for 12 d, the thylakoid membranes were isolated, membrane proteins (10 μg) were separated by SDS-PAGE (lower panel), and subjected to western blotting (upper panel) probed with D1-, CP47-, PsaA/B-, and PsaC-specific antibodies.
C. P_{700} oxidation measured as the change in absorbance at 705 nm under actinic light (320 μmol photons m^{-2} s^{-1}); 20 μM 3-(3,4-dichlorophenyl)-1,1-dimethylurea (DCMU) was added to block PSII activity.
D, E. P_{700}^{+} reduction curves of *N. sphaeroides* treated with DCMU and methyl viologen (MV); 20 μM DCMU was used to disrupt the linear electron flow; 2 mM MV was used as an efficient PSI electron acceptor to block the cyclic electron flow. Data are means ± SD (n = 5–6).

12 days exposure to low UV-B radiation (t-test, $P > 0.05$). To gain further insight into the response of the PSII acceptor side to low UV-B radiation, we measured the kinetics of chlorophyll fluorescence relaxation following single turnover or multiple turnover flashes to evaluate the time constant for electron transport on the PSII acceptor side (τ_{Qa}) or between PSII and PSI (τ_{PQ}), respectively. Compared with the control, which was exposed to PAR only, the τ_{Qa} and τ_{PQ} values for UV-B-treated samples were significantly decreased by 62% and 50% (t-test, $P < 0.05$), which indicated that both Q_A and PQ pool reoxidation were more rapid in UV-B-acclimated samples.

Table 1. Rate constants for P_{700}^+ reduction of *Nostoc sphaeroides* treated with 3-(3,4-dichlorophenyl)-1,1-dimethylurea (DCMU) and methyl viologen (MV) after 12 days exposure to photosynthetically active radiation (PAR) or PAR plus UV-B radiation.

	P_{700}^+ reduction rate (k, s^{-1})	
Inhibitors used	Non-UV-B acclimated	UV-B acclimated
No inhibitors	18.13 ± 7.34[a]	20.52 ± 4.41[a]
+ DCMU	0.99 ± 0.13[a]	2.21 ± 0.23[b]
+ DCMU + MV	0.46 ± 0.05[a]	0.60 ± 0.11[b]

Final concentrations of inhibitors were 20 μM DCMU and 2 mM MV. Values followed by different superscript letters for the same treatment are significantly different (t-test, $P < 0.05$). Data are means ± SD (n = 5–8).

Low UV-B acclimation enhanced the photosynthetic capacity of N. sphaeroides

To estimate photosynthetic capacity, we measured the photosynthetic responses to irradiance for *N. sphaeroides*. As light intensity increases, the photosynthetic rates of UV-B acclimated samples increased more rapidly than those of the non-acclimated control (Fig. 4A). Specifically, the light-saturated photosynthetic rate (P_{max}) and the light-limited photosynthetic efficiency (α) of UV-B acclimated samples were significantly enhanced by 47% and 54%, respectively, compared with those of the non-acclimated control (t-test, $P < 0.05$).

UV-B acclimated N. sphaeroides *were more resistant to subsequent strong UV-B and high-light treatments*

The maximal PSII quantum yield of UV-B acclimated and non-acclimated *N. sphaeroides* were measured during subsequent strong UV-B and high-light treatments. When exposed to 1 W m^{-2} UV-B for 5 h, the F_v/F_m values of UV-B acclimated and non-acclimated colonies continuously decreased, to 30% and 22% of the initial values, respectively. This result indicated that UV-B-induced photoinhibition in UV-B-acclimated colonies was ameliorated under UV-B stress. In the presence of the protein synthesis inhibitor lincomycin, the F_v/F_m values declined sharply to similar levels (about 20% of the initial values), suggesting that PSII damage in both UV-B acclimated and non-acclimated colonies was affected to a similar extent. In addition, UV-B-acclimated cells exhibited faster *de novo* protein synthesis for PSII repair under strong UV-B radiation, as was evident from the greater reduction in F_v/F_m value in the absence and presence of lincomycin (Fig. 4B).

Similar effects in alleviation of photoinhibition were observed following high-light treatment (Fig. 4C). Specifically, during 3 h exposure to 500 μmol photons m^{-2} s^{-1}, the F_v/F_m value first decreased drastically, then remained stable at up to 39% and 25% of the initial values for UV-B acclimated and non-acclimated colonies, respectively, in the absence of lincomycin. The F_v/F_m value showed a more strongly significant decrease for UV-B acclimated and non-acclimated colonies with the addition of lincomycin, and attained similar levels (11%–14% of the initial values).

Since PSII repair is closely linked to the turnover of PSII core protein D1 during photoinhibition, we measured levels of the D1 protein (Fig. 4D and E). In agreement with UV-B or HL-induced photoinhibition, levels of D1 were reduced following UV-B stress or HL exposure (Fig. 4D; 'Non-acclimated'). However, D1 levels in acclimated colonies decreased less following UV-B stress or HL exposure (Fig. 4D; 'UV-B acclimated'). We further found that the addition of lincomycin equalized the effect that UV-B stress or HL-exposure had on nonacclimated and acclimated colonies, with equal and larger reduction in D1 levels observed for both samples (Fig. 4E; 'UV-B acclimated' versus 'Non-acclimated'). The dynamics of D1 protein levels in these experiments were consistent with UV-B stress or HL-induced photoinhibition monitored by measuring *Fv*/*Fm*. These results indicated that the alleviation of photoinhibition in UV-B acclimated *N. sphaeroides* is associated with the induction of faster rates of D1 resynthesis.

Discussion

Low-dose UV-B can act as a positive ecological factor

Although UV radiation (UVR) is usually viewed as a negative environmental factor (Häder et al. 2015), positive effects of UVR have been reported, with the predominant focus on UV-A (315–400 nm). Ultraviolet-A radiation has been suggested to be capable of driving primary production of certain large marine phytoplankton species on cloudy days or under reduced solar radiation (Barbieri et al. 2002; Wu et al. 2005; Gao et al. 2007; Xu and Gao 2010; Li and Gao 2013), although the mechanisms underpinning positive effects remain largely unclear. Some researchers have noted that UV-A energy can be utilized for carbon fixation because the absorption spectrum of Chl *a* extends into the UV band and thus Chl *a* absorbs a proportion of UV-A radiation (McLeod and Kanwisher 1962; Halldall 1964; Xu and Gao 2016). In the present study, we observed that the low UVR-mediated positive effect under low visible light was attributed to UV-B (0.08 W m^{-2}) rather than UV-A, because low-dose UV-A (0.33 W m^{-2}) from the UV-B lamp did not affect growth of *N. sphaeroides* (Supporting Information Fig. S1), compared to that exposed to low visible light alone (4.35 W m^{-2}). In previous studies, positive effects of UV-B on photosynthetic organisms have only been observed

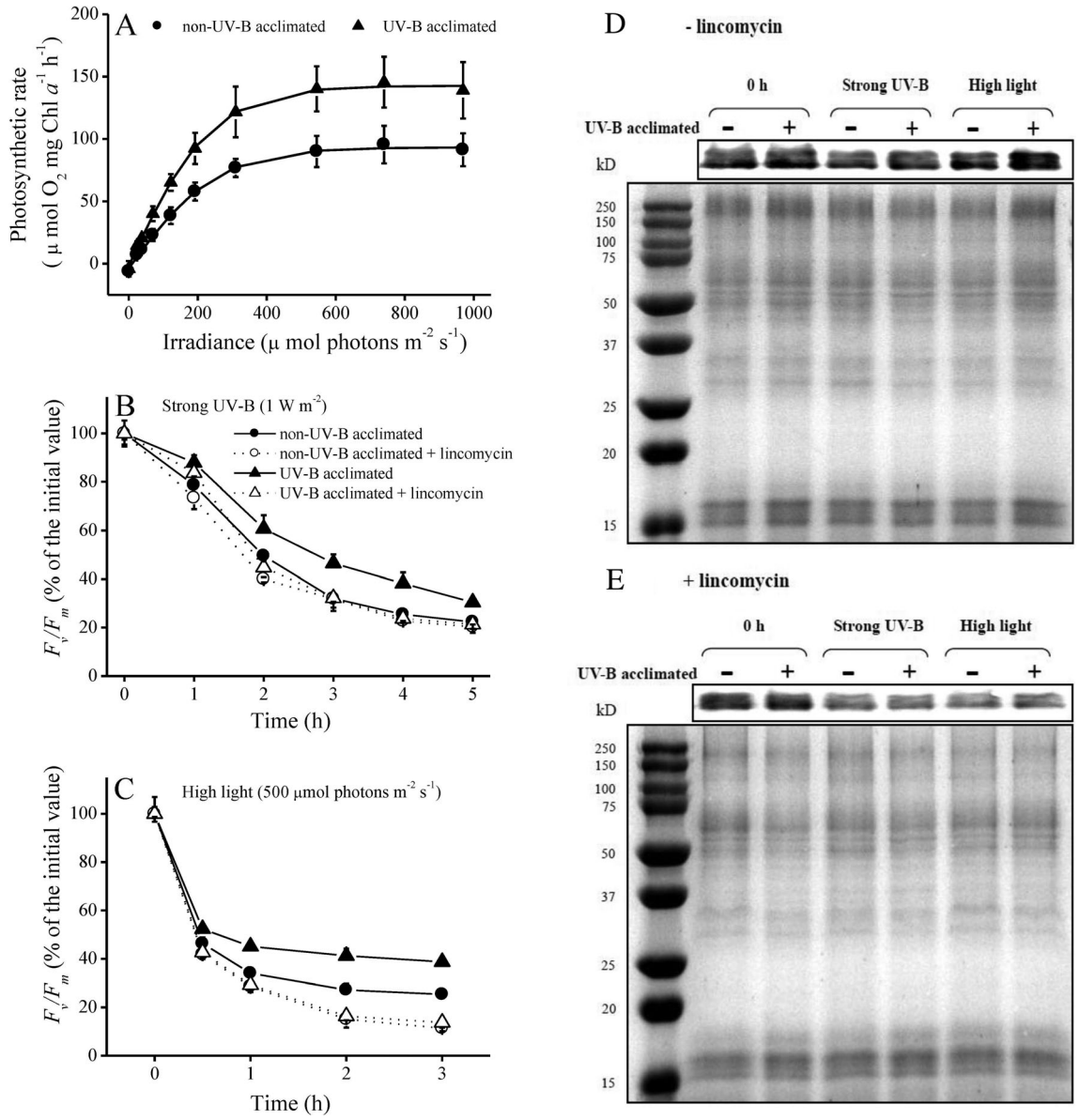

Fig. 4. Effects of 12 days exposure to UV-B radiation on photosynthesis and photoinhibition of *Nostoc sphaeroides*.
A. Photosynthetic response to irradiance (P–I) curves. Data are means ± SD (n = 4–5).
B, C. Changes in maximal photosystem II (PSII) photochemical quantum yield during strong UV-B radiation and high-light treatments in *N. sphaeroides* after 12 days exposure to photosynthetically active radiation (PAR) or PAR plus UV-B. During the experiment, samples were treated without or with 0.1 g L^{-1} lincomycin. The 100% of *Fv*/*F*m values was 0.45 ± 0.02, 0.45 ± 0.01, 0.44 ± 0.02, and 0.44 ± 0.02 before exposure to strong UV-B, 0.44 ± 0.01, 0.47 ± 0.01, 0.43 ± 0.03, and 0.45 ± 0.02 before exposure to high light, respectively, for non-acclimated, non-acclimated + lincomycin, UV-B-acclimated, UV-B-acclimated + lincomycin samples. For lincomycin treatment, samples were first treated with lincomycin for 20 min in the darkness and then transferred to strong UV-B or HL treatments. Data are means ± SD (n = 5–6).
D, E. Western blot analysis of D1 protein levels in UV-B acclimated and non-acclimated colonies before and following 3 h strong UV-B exposure or 2 h high light treatments, in the absence or presence of lincomycin. +: UV-B acclimated colonies; –: non-UV-B acclimated colonies. The D1 level was determined using a commercially available polyclonal antibody. For SDS-PAGE (lower panel) and Western blot (upper panel), equal amounts of protein samples, 20 μg per lane, were loaded on 12% polyacrylamide gels.

when the dose is lower than 10 kJ m^{-2} d^{-1} (about 0.1 W m^{-2} if given constant exposure per day) (Supporting Information Table S1). Such low intensities of UV-B radiation are widely present in nature, such as at high latitudes (*e.g.* 10 kJ m^{-2} d^{-1}, 53° N, 1° W), certain water depths (*e.g.* lower than 0.1 W m^{-2} UV-B at water depths of more than 7 m in the South China Sea with lower than 100 W m^{-2} PAR, 16°51′ N, 112°20′ E), or shaded habitats (*e.g.* UV-B penetration through a closed forest canopy can be as little as 1%–2%) (Hargreaves

2003; Paul and Gwynn-Jones 2003; Li et al. 2013). In colony-forming cyanobacteria with a polysaccharide sheath, such as *N. sphaeroides* and *N. flagelliforme* (Fig. 1; Supporting Information Table S1) (Deng et al. 2008; Feng et al. 2012), the inner gelatinous matrix represents a niche of low UV-B radiation and weak visible light because of intercellular self-shading (Raven and Kübler 2002; Gao and Ai 2004; Aguilar et al. 2019). Low-dose UV-B can be unavoidably perceived by photosynthetic organisms in these niches, and a small number of studies have reported positive effects of UV-B radiation on photosynthetic eukaryotes (Supporting Information Table S1). However, the effects of UV-B on photosynthetic prokaryotes remain largely unknown. The present data suggested that low-dose UV-B can act as a positive ecological factor for the productivity of the photosynthetic prokaryote *N. sphaeroides*.

A novel mechanism of photosynthetic acclimation to low-dose UV-B

It has been extensively reported that UV-B can stimulate protective responses quickly to offset possible negative impacts because of its high energy and damage potential (Jiang and Qiu 2011; Shang et al. 2018). Our previous findings demonstrated that 2 h UV-B radiation stimulated significant increases in contents of the photoprotective carotenoid pigments in *Microcystis aeruginosa* (Jiang and Qiu 2011), and 54 h of UV-B treatment increased by 2 times the MAAs content of *N. flagelliforme* (Shang et al. 2018). The present study showed that MAAs accumulation in *N. sphaeroides* was rapidly induced and attained 1.6 times that of the control during 4 days exposure to low UV-B radiation (Fig. 2D). However, the synthesis of these photoprotective substances requires additional energy, and thus these results cannot explain the increase in the growth rate and biomass production of *N. sphaeroides* under low-dose UV-B treatment. Low UV-B radiation must initiate unknown mechanisms to readjust the photosynthetic apparatus to enhance photosynthetic efficiency for increased ATP or NADPH production and offset the energy consumption for biosynthesis of photoprotective substances. Thus, low UV-B radiation probably functions as a crucial environmental cue and activates currently unidentified signalling components to regulate the photophysiological state of cyanobacterial species. Although the UV-B photoreceptor has not been identified in cyanobacteria and their UV-B signal transduction is poorly understood, we strongly suggest that low UV-B radiation may adjust photosystem content and photosynthetic electron transport to improve the photosynthetic capacity and biomass production of *N. sphaeroides*, as detailed below.

It is commonly accepted that PSII is the major target of UV-B impairment because the oxygen-evolving complex is highly sensitive to UV-B (Takahashi et al. 2010; Jiang and Qiu 2011; Kataria et al. 2014). However, in the present study, PSII content and PSII activity ($H_2O \rightarrow p$-BQ) were not influenced after 12 days exposure to UV-B. The possible damage to the PSII complex caused by low-dose UV-B could be counteracted by acceleration of the PSII repair cycle (Fig. 4) (Wu et al. 2011). In contrast to PSII, PSI is less sensitive to UV-B (Kulandaivelu and Noorudeen 1983), and is only impaired when exposed to a high intensity of UV-B radiation (Renger et al. 1982). The present results revealed enhanced accumulation of PSI in thylakoid membranes of UV-B acclimated *N. sphaeroides*, which contributed to the increase in the PSI/PSII ratio after 8 days exposure to low UV-B radiation.

The adjustment of photosystem stoichiometry is a well-documented acclimation response to maintain effective photosynthetic energy conversion under varying visible light environments in cyanobacteria (Herranen et al. 2005). The changes in PSI/PSII ratio result mainly from regulation of PSI abundance (Fujita et al. 1985; Aizawa et al. 1992; Hihara et al. 1998). Upon transfer to high light conditions, cyanobacteria can decrease photosystem content in avoidance of absorbing excess light energy, and the main down-regulated component is PSI rather than PSII (Murakami and Fujita 1991; Hihara et al. 1998). In contrast, under low light conditions, cyanobacteria increase the PSI/PSII ratio, and especially the PSI content, to up-regulate light harvesting capacity (Van Liere and Walsby 1982; Kopečná et al. 2012). The mechanism responsible for the changes in PSI content is not clear; however, the process appears to be tightly associated with the chlorophyll biosynthetic pathway (Jordan et al. 2001; Kopečná et al. 2012). Chlorophyll synthesis regulation depends on a signal, which could be the redox state (Murakami and Fujita 1993; Herranen et al. 2005). It is likely that the regulatory mechanism of PSI content induced by low-dose UV-B is positively coupled to the regulation during exposure to low visible light. Low UV-B acclimation could further promote the accumulation of PSI content under low light conditions in *N. sphaeroides*, although elucidation of the specific regulatory mechanism needs further investigation.

Electron flux through the photosynthetic electron transport chain was recently reported to limit the photosynthetic rate in *Synechococcus* PCC 7942 compared with the fastest growing *Synechococcus* UTEX 2973 at various light intensities (Ungerer et al. 2018). A high amount of PSI has been reported to accelerate the rate of photosynthetic electron transport (Hihara et al. 1998) and promote photosynthetic efficiency, because increased PSI content can provide greater oxidizing power to accept electrons from PSII and alleviate the downstream bottleneck

Table 2. Effects of 12 days exposure to UV-B radiation on photosystem II (PSII) function of *Nostoc sphaeroides*.

Parameters	Non-UV-B acclimated	UV-B acclimated
PSII activity ($H_2O \rightarrow p$-BQ) (μmol O_2 mg Chl a^{-1} h^{-1})	255.25 ± 48.93[a]	248.39 ± 67.83[a]
F_v/F_m	0.47 ± 0.03[a]	0.46 ± 0.04[a]
τ_{Qa} (μs)	344.0 ± 80.8[a]	129.3 ± 1.3[b]
τ_{PQ} (μs)	15767.6 ± 1695.6[a]	7848.0 ± 2551.6[b]

F_v/F_m: the maximal quantum yield of PSII photochemistry; τ_{Qa}: the time constant for electron transport on the PSII acceptor side; τ_{PQ}: the time constant for electron transport between PSII and PSI. Values followed by different superscript letters for the same parameter are significantly different (*t*-test, $P < 0.05$). Data are means ± SD ($n = 4–8$).

limitation in the electron transport chain (Ungerer et al. 2018). In the present study, UV-B acclimated and non-acclimated samples showed similar PSII contents and maximal photosynthetic capacities of PSII (Fig. 3; Table 2) and are likely to be capable of sending a similar number of electrons from PSII under saturating light. An increase in PSI content in UV-B-acclimated samples led to higher oxidizing photochemical activity of PSI (Fig. 3), which served to empty electrons out of PSII more efficiently as indicated by the faster Q_A reoxidation and PQ pool reoxidation (Table 2). This feature resulted in enhanced photosynthetic efficiency (α) and higher light-saturated oxygen evolution rate (P_{max}) (Fig. 4) in UV-B-acclimated samples. Enhanced Q_A reoxidation could be due to cyclic PSII electron transport, which can protect the desiccation-tolerant filamentous cyanobacterium *Microcoleus vaginatus* against photodamage under excess illumination (Ohad et al. 2010). However, both UV-B acclimated and non-acclimated samples were cultured under low visible light conditions, and PSII photodamage was not observed in UV-B acclimated colonies in the present study. Thus, faster drawing of electrons from PSII in UV-B acclimated colonies was resulted from the increase of PSI content. Compared with the samples exposed to PAR alone, the UV-B acclimated colonies acquired a one-fold higher cyclic electron transfer rate around PSI (Fig. 3; Table 1). Cyclic electron transfer around PSI is an important source of ATP production in cyanobacteria because it can promote the proton transport from cytosol to thylakoid lumen, which can enhance the ADP phosphorylation driven by the proton return flux (Thomas et al. 2001; Yamori and Shikanai 2016). Cyclic electron transfer around PSI is important for the growth of cyanobacteria at low light intensities. *Synechococcus* sp. PCC 7002 mutants lacking this pathway grew well under optimal conditions but more slowly than the wild type under weak light (Yu et al. 1993). The enhancement of cyclic electron transfer around PSI in UV-B acclimated *N. sphaeroides* can provide additional ATP for chlorophyll synthesis and PSI accumulation, which could improve light harvesting capacity under low light conditions. Thus, the increase in photosynthetic capacity coinciding with elevated cyclic electron transfer around PSI may contribute to the enhancement of growth and biomass production in UV-B acclimated colonies (Fig. 5). These findings demonstrated for the first time that low-dose UV-B induces cyanobacteria to achieve efficient photosynthesis and exerts a positive effect on growth and biomass production by enhancing PSI content and cyclic electron transfer around PSI (Fig. 5).

Ecological significance of low-dose UV-B

Nostoc sphaeroides is a representative nitrogen-fixing cyanobacterium with a gelatinous polysaccharide sheath (Gao and Ai 2004; Fig. 1). This type of cyanobacteria seems to be more tolerant to UV-B than other photosynthetic organisms (Ehling-Schulz et al. 1997; Helbling et al. 2006; Shang et al. 2018), because sunscreen compounds within the sheath can shield UV-B radiation and the inner cells receive low-dose or non-damaging UV-B radiation (Raven and Kübler 2002; Gao and Ai 2004). This type of nitrogen-fixing cyanobacteria, which includes *N. sphaeroides*, *N. flagelliforme*, and *N. commune*, shows a widespread distribution and plays an important role in the contribution of primary production and carbon/nitrogen biogeochemical cycles in diverse habitats (Novis et al. 2007; Sand-Jensen 2014). The novel source of nitrogen from nitrogen-fixing cyanobacteria has been reported to be an important biological fertilizer and promotes the microbial community of rice fields and in soils of other agro-ecosystems. With the gradual recovery of the stratospheric ozone layer, the UV-B dosage is decreasing, and the positive effects of low UV-B radiation on the productivity of sheathed cyanobacteria will be gradually enhanced in the future.

N. sphaeroides is a typical low-light adapted cyanobacterium. This type of low-light adapted cyanobacteria is widespread and abundant in nature because they can synthesize specific light-harvesting complexes or significantly greater amounts of chlorophyll to adapt to low light (Van Liere and Walsby 1982; Wiethaus et al. 2010; Kopečná et al. 2012). For instance, the marine cyanobacterium *Prochlorococcus* is present from the water surface to a depth of ~150 m in the open ocean between 40° N and 40° S and has evolved low-light ecotypes (Partensky et al. 1999). This cyanobacterium contributes significantly to primary production and its annual mean global abundance attains $2.9 \pm 0.1 \times 10^{27}$ cells (Flombaum et al. 2013). Biologically effective doses of UV radiation have been detected to an underwater depth of 70 m (Smith et al. 1992), and the dose of UV-B can be lower than

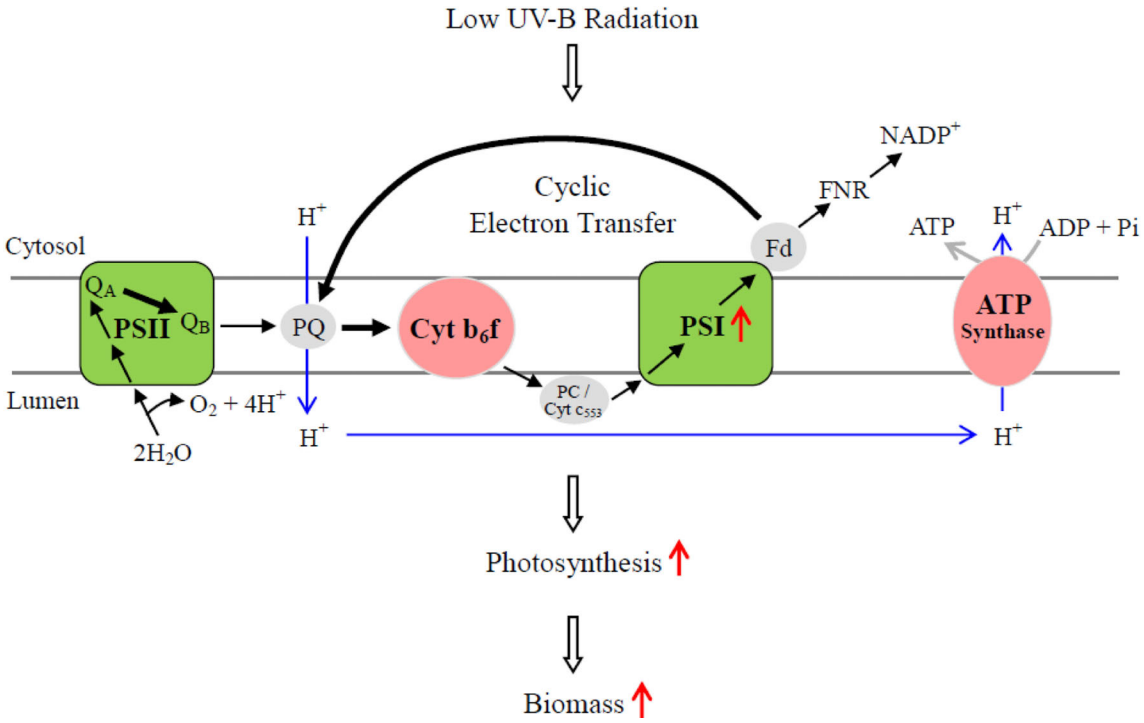

Fig. 5. The model of photosynthetic acclimation to low-dose UV-B radiation in *Nostoc sphaeroides*. Low-dose UV-B induced *N. sphaeroides* to increase photosynthesis under low visible light and exerted a positive effect on biomass production by enhancing the primary quinone-type acceptor (Q_A) re-oxidation, plastoquinone (PQ) pool re-oxidation, photosystem I (PSI) content and cyclic electron transfer around PSI.

0.1 W m^{-2} at a depth of more than 7 m in sea water (16°51′ N, 112°20′ E) (Li et al. 2013). Thus, a large number of marine photosynthetic prokaryotes may be affected by low UV-B radiation. Based on the novel photosynthetic acclimation mechanism to UV-B radiation discussed above, we assume that the positive effect of low-dose UV-B on photosynthetic output is universal among cyanobacteria under various low-light environments, and the contribution of low UV-B radiation to global primary productivity might be greatly under-estimated.

Experimental procedures

Materials and culture conditions

Nostoc sphaeroides is a colony-forming and nitrogen-fixing cyanobacterium distributed in rice fields (Qiu et al. 2002). The samples we used in this study were originally collected from Hefeng County in Hubei Province, People's Republic of China. Axenic *N. sphaeroides* cultures were isolated with serial dilution and plate streaking in BG11 medium under weak fluorescent light irradiation. Subcultures were prepared and incubated in nitrogen-free $BG11_0$ medium at 25 °C and aerated with filtered air (Millipore, 0.22 μm). Illumination was provided by cool-white fluorescent lights with a photon flux density of 20 μmol photons m^{-2} s^{-1} (equal to 4.35 W m^{-2} according to Neale et al. 2001). UV-B radiation was supplied by a fluorescent UV-B lamp (TL 40W/12RS; Philips, Cologne, Germany) synchronized with photosynthetic active radiation (PAR). The lamp's emission spectrum was measured with a scanning spectroradiometer (SPR-920; Sanse Instrument Ltd, Zhejiang, China) (Supporting Information Fig. S2A). Ultra white glass was used to filter radiation below 280 nm (Supporting Information Fig. S2B). According to the biological spectral weighting function of Flint and Caldwell (2003), 0.08 W m^{-2} biologically effective UV-B radiation was provided for the UV-B-treated samples (Supporting Information Fig. S2C). Samples were cultivated in a quartz conical flask for UV-B treatments. Samples cultured without UV-B radiation were used as the control. Hormogonia of *N. sphaeroides* were obtained from the spherical colony in accordance with the method of Li et al. (2005). The inoculi contained 30 μg L^{-1} chlorophyll *a* (Chl *a*) for the following experiments.

Growth measurement and UV-absorbing compound assay

The samples in liquid culture were harvested by centrifugation at 6000 × *g* for 10 min and extracted with 100% methanol overnight at 4 °C for MAAs (Helbling et al. 2006; Ishihara et al. 2017). The extracts were scanned

with a Cary 300 UV–VIS spectrophotometer (Varian Australia Pty Ltd, Mulgrave, Australia) from 250 to 750 nm. The concentration of Chl *a* was calculated as described by Lichtenthaler and Buschmann (2001). The content of MAAs was determined from the ratio of the absorbance at 334 nm (MAAs) to 665 nm (Chl *a*) in accordance with the method of Ishihara et al. (2017). Specific growth rate (μ) was calculated with the following equation: $\mu = (\ln X_2 - \ln X_1)/(T_2 - T_1)$, where X_1 and X_2 are Chl *a* contents at times T_1 and T_2, respectively. The samples from liquid culture were heated at 105 °C until constant weight, and the dry weight (DW) was determined.

Measurement of chlorophyll fluorescence

Maximal photosystem II (PSII) photochemical quantum yield (F_v/F_m) was determined using a plant efficiency analyser (Hansatech Instruments, King's Lynn, UK). All samples were dark adapted for 10 min before measurements (Campbell et al. 1998). Photosynthetic performance of cultures was assayed further with a fluorescence induction and relaxation fluorometer system (Satlantic Inc., Halifax, NS, Canada) as described by Liu and Qiu (2012). The rate constant for relaxation of the primary quinone-type acceptor (Q_A) or plastoquinone (PQ) was the first one retrieved from a three-component exponential kinetic analysis (Kolber et al. 1998). The 77 K fluorescence emission spectra of the samples were measured with a Hitachi F-4500 fluorescence spectrophotometer (Hitachi High-Technologies Co., Tokyo, Japan) as described by Volkmer et al. (2007) using an excitation wavelength of 435 nm. All samples were at a concentration of about 3 μg Chl *a* mL^{-1}. The PSI/PSII fluorescence ratio was obtained by comparing the relative fluorescence intensity readings at 725 and 685 nm in accordance with the method of Murakami (1997). The fluorescence spectra were normalized at 685 nm (the fluorescence emission peak of PSII).

To estimate photosystem I (PSI) photochemical activity, the samples were adjusted to the same fresh weight (0.015 g) and distributed on a glass fibre membrane for measurements. The P_{700} oxidation kinetics were measured as the absorbance change at 705 nm under actinic light (320 μmol photons m^{-2} s^{-1}) in the presence of 20 μM 3-(3,4-dichlorophenyl)-1,1-dimethylurea (DCMU) with a Joliot JTS-10 spectrophotometer (BioLogic Science Instruments, Grenoble, France) as described previously (Salomon and Keren 2011). The P_{700}^+ reduction kinetics was measured in accordance with the method of Alric et al. (2010). To determine the cyclic electron flow, 20 μM DCMU was added to the samples prior to measurements. Methyl viologen (MV; 2 mM) was used to block the cyclic electron flow in the presence of DCMU (Yu et al. 1993).

Measurement of photosynthetic oxygen evolution

The photosynthetic oxygen evolution of samples was monitored using a Clark-type oxygen electrode (Chlorolab 2, Hansatech Instruments) at 25 °C. The PSII activity was determined at 550 μmol photons m^{-2} s^{-1} with H_2O as the electron donor and *p*-benzoquinone (*p*-BQ) as the electron acceptor in the presence of 1 mM *p*-BQ and 1 mM potassium ferricyanide. During the irradiance-dependent photosynthetic measurement, the samples harvested were resuspended in fresh $BG11_0$ medium buffered with 25 mM bis-tris propane (pH 8.0), supplemented with 2 mM $NaHCO_3$ to avoid carbon limitation. Parameters for the photosynthetic response to irradiation were analysed in accordance with Henley (1993): $P = P_{max} \times \tanh(\alpha \times I / P_{max}) + R_d$, where I is irradiance; P is photosynthetic activity at a specific irradiance; P_{max} is light-saturated photosynthesis; the ascending slope at limiting irradiances, α, is a function of both light-harvesting efficiency and photosynthetic energy conversion efficiency, which represents the photosynthetic efficiency; and R_d is dark respiration.

Western blot analysis

To isolate thylakoid membranes, samples were pulverized in liquid N_2 to obtain a homogeneous powder and suspended in ice-cold isolation buffer containing 25% glycerol, 50 mM Mes-NaOH (pH 6.5), 5 mM $CaCl_2$, 10 mM $MgCl_2$, and 1 mM phenylmethylsulfonyl fluoride (PMSF). Cells were ruptured with a UP200S ultrasonic processor (Hielscher Ultrasound Technology, Teltow, Germany) in an ice bath for 10 min at 40% amplitude and a 30% duty cycle. Cell debris and unbroken cells were removed by centrifugation at 4000 × *g* and 4 °C for 10 min. Total thylakoid membrane proteins and cytosolic soluble proteins were separated by centrifugation at 40,000 × *g* and 4 °C for 60 min. The resulting thylakoids were resuspended in isolation buffer and used for Western blot analysis. SDS-PAGE and Western blotting were performed using standard methods. Briefly, equal amounts of proteins (10 μg) were loaded, separated by 12% SDS-PAGE, transferred to nitrocellulose filters (Millipore, Carrigtohill, Ireland), detected with PsaA/B-, PsaC-, CP47- and D1-specific primary antibodies, and visualized with goat anti-rabbit alkaline phosphatase antibody with nitroblue tetrazolium and 5-bromo-4-chloro-3-indolylphosphate (Amresco) as the substrates. The target proteins were detected and visualized by chemiluminescence using the FluoChem R system (ProteinSimple, Santa Clara, CA, USA).

Photoinhibition treatment

To determine the chlorophyll fluorescence of *N. sphaeroides* during strong UV-B and high light treatments, samples were

placed in culture dishes and illuminated with 1 W m^{-2} UV-B for 5 h or 500 μmol photons m^{-2} s^{-1} for 3 h, respectively. The temperature was maintained at 25 °C. Samples were taken at different intervals to determine the maximal PSII photochemical quantum yield (F_v/F_m). The F_vF_m value of non-photoinhibited colonies was considered to be 100% to calculate the degree of photoinhibition. Lincomycin (0.1 g L^{-1}) was used to block cyanobacterial protein translation.

Acknowledgements

This study was funded by the National Natural Science Foundation of China (Nos. 31670332 and 31170309).

Competing financial interests

The authors declare no competing financial interests.

References

Aguilar, P., Dorador, C., Vila, I., and Sommaruga, R. (2019) Bacterial communities associated with spherical *Nostoc* macrocolonies. *Front Microbiol* **10**: 483.

Aizawa, K., Shimizu, T., Hiyama, T., Satoh, K., Nakamura, Y., and Fujita, Y. (1992) Changes in composition of membrane proteins accompanying the regulation of PSI/PSII stoichiometry observed with *Synechocystis* PCC 6803. *Photosynth Res* **32**: 131–138.

Allorent, G., Lefebvre-Legendre, L., Chappuis, R., Kuntz, M., Truong, T.B., Niyogi, K.K., *et al*. (2016) UV-B photoreceptor-mediated protection of the photosynthetic machinery in *Chlamydomonas reinhardtii*. *Proc Natl Acad Sci U S A* **113**: 14864–14869.

Alric, J., Lavergne, J., and Rappaport, F. (2010) Redox and ATP control of photosynthetic cyclic electron flow in *Chlamydomonas reinhardtii* (I) aerobic conditions. *Biochim Biophys Acta* **1797**: 44–51.

Bais, A.F., McKenzie, R.L., Bernhard, G., Aucamp, P.J., Ilyas, M., Madronich, S., and Tourpali, K. (2015) Ozone depletion and climate change: impacts on UV radiation. *Photochem Photobiol Sci* **14**: 19–52.

Barbieri, E.S., Villafañe, V.E., and Helbling, E.W. (2002) Experimental assessment of UV effects on temperate marine phytoplankton when exposed to variable radiation regimes. *Limnol Oceanogr* **47**: 1648–1655.

Brown, B.A., Cloix, C., Jiang, G.H., Kaiserli, E., Herzyk, P., Kliebenstein, D.J., and Jenkins, G.I. (2005) A UV-B-specific signaling component orchestrates plant UV protection. *Proc Natl Acad Sci U S A* **102**: 18225–18230.

Cai, X.N., Hutchins, D.A., Fu, F.X., and Gao, K.S. (2017) Effects of ultraviolet radiation on photosynthetic performance and N_2 fixation in *Trichodesmium erythraeum* IMS 101. *Biogeosciences* **14**: 4455–4466.

Campbell, D., Hurry, V., Clarke, A.K., Gustafsson, P., and Öquist, G. (1998) Chlorophyll fluorescence analysis of cyanobacterial photosynthesis and acclimation. *Microbiol Mol Biol Rev* **62**: 667–683.

Chen, J.J., Mitchell, D.L., and Britt, A.B. (1994) A light-dependent pathway for the elimination of UV-induced pyrimidine (6-4) pyrimidinone photoproducts in *Arabidopsis*. *Plant Cell* **6**: 1311–1317.

Chipperfield, M.P., Bekki, S., Dhomse, S., Harris, N.R.P., Hassler, B., Hossaini, R., *et al*. (2017) Detecting recovery of the stratospheric ozone layer. *Nature* **549**: 211–218.

Deng, Z., Hu, Q., Lu, F., Liu, G., and Hu, Z. (2008) Colony development and physiological characterization of the edible blue-green alga, *Nostoc sphaeroides* (Nostocaceae, Cyanophyta). *Prog Nat Sci* **18**: 1475–1483.

Ehling-Schulz, M., Bilger, W., and Scherer, S. (1997) UV-B-induced synthesis of photoprotective pigments and extracellular polysaccharides in the terrestrial cyanobacterium *Nostoc commune*. *J Bacteriol* **179**: 1940–1945.

Feng, Y.N., Zhang, Z.C., Feng, J.L., and Qiu, B.S. (2012) Effects of UV-B radiation and periodic desiccation on the morphogenesis of the edible terrestrial cyanobacterium *Nostoc flagelliforme*. *Appl Environ Microb* **78**: 7075–7081.

Flint, S.D., and Caldwell, M.M. (2003) A biological spectral weighting function for ozone depletion research with higher plants. *Physiol Plant* **117**: 137–144.

Flombaum, P., Gallegos, J.L., Gordillo, R.A., Rincón, J., Zabala, L.L., Jiao, N., *et al*. (2013) Present and future global distributions of the marine cyanobacteria *Prochlorococcus* and *Synechococcus*. *Proc Natl Acad Sci U S A* **110**: 9824–9829.

Fujita, Y., Ohki, K., and Murakami, A. (1985) Chromatic regulation of photosystem composition in the photosynthetic system of red and blue-green algae. *Plant Cell Physiol* **26**: 1541–1548.

Gao, K., and Ai, H. (2004) Relationship of growth and photosynthesis with colony size in an edible cyanobacterium, Ge-Xian-Mi *Nostoc* (Cyanophyceae). *J Phycol* **40**: 523–526.

Gao, K., Wu, Y., Li, G., Wu, H., Villafañe, V.E., and Helbling, E.W. (2007) Solar UV radiation drives CO_2 fixation in marine phytoplankton: a double-edged sword. *Plant Physiol* **144**: 54–59.

Häder, D.P., Williamson, C.E., Wängberg, S.Å., Rautio, M., Rose, K.C., Gao, K., *et al*. (2015) Effects of UV radiation on aquatic ecosystems and interactions with other environmental factors. *Photochem Photobiol Sci* **14**: 108–126.

Halldall, P. (1964) Ultraviolet action spectra of photosynthesis and photosynthetic inhibition in a green and a red alga. *Physiol Plant* **17**: 414–421.

Hargreaves, B.R. (2003) Water column optics and penetration of UVR. In *UV Effects in Aquatic Organisms and Ecosystems*, Helbling, E.W., and Zagarese, H.E. (eds). Amsterdam, Netherlands: Elsevier, pp. 59–105.

Helbling, E.W., Gao, K., Ai, H., Ma, Z., and Villafañe, V.E. (2006) Differential responses of *Nostoc sphaeroides* and *Arthrospira platensis* to solar ultraviolet radiation exposure. *J Appl Phycol* **18**: 57–66.

Henley, W.J. (1993) Measurement and interpretation of photosynthetic light-response curves in algae in the context of photoinhibition and diel changes. *J Phycol* **29**: 729–739.

Herranen, M., Tyystjärvi, T., and Aro, E.M. (2005) Regulation of photosystem I reaction center genes in *Synechocystis* sp. strain PCC 6803 during light acclimation. *Plant Cell Physiol* **46**: 1484–1493.

Hihara, Y., Sonoike, K., and Ikeuchi, M. (1998) A novel gene, *pmgA*, specifically regulates photosystem stoichiometry in the cyanobacterium *Synechocystis* sp. PCC

6803 in response to high light. *Plant Physiol* **117**: 1205–1216.

Ishihara, K., Watanabe, R., Uchida, H., Suzuki, T., Yamashita, M., Takenaka, H., *et al*. (2017) Novel glycosylated mycosporine-like amino acid, 13-*O*-(β-galactosyl)-porphyra-334, from the edible cyanobacterium *Nostoc sphaericum* - protective activity on human keratinocytes from UV light. *J Photochem Photobiol B* **172**: 102–108.

Jenkins, G.I. (2009) Signal transduction in responses to UV-B radiation. *Annu Rev Plant Biol* **60**: 407–431.

Jiang, H.B., and Qiu, B.S. (2011) Inhibition of photosynthesis by UV-B exposure and its repair in the bloom-forming cyanobacterium *Microcystis aeruginosa*. *J Appl Phycol* **23**: 691–696.

Jordan, P., Fromme, P., Witt, H.T., Klukas, O., Saenger, W., and Krauβ, N. (2001) Three-dimensional structure of cyanobacterial photosystem I at 2.5 Å resolution. *Nature* **411**: 909–917.

Kataria, S., Jain, K., and Guruprasad, K.N. (2007) UV-B induced changes in antioxidant enzymes and their isoforms in cucumber (*Cucumis sativus L*.) cotyledons. *Indian J Biochem Biol* **44**: 31–37.

Kataria, S., Jajoo, A., and Guruprasad, K.N. (2014) Impact of increasing ultraviolet-B (UV-B) radiation on photosynthetic processes. *J Photochem Photobiol B* **137**: 55–66.

Kerr, J.B., and McElroy, C.T. (1993) Evidence for large upward trends of ultraviolet-B radiation linked to ozone depletion. *Science* **262**: 1032–1034.

Kolber, Z.S., Prasil, O., and Falkowski, P.G. (1998) Measurements of variable chlorophyll fluorescence using fast repetition rate techniques: defining methodology and experimental protocols. *Biochim Biophys Acta* **1367**: 88–106.

Kopečná, J., Komenda, J., Bučinská, L., and Sobotka, R. (2012) Long-term acclimation of the cyanobacterium *Synechocystis* sp. PCC 6803 to high light is accompanied by an enhanced production of chlorophyll that is preferentially channeled to trimeric photosystem I. *Plant Physiol* **160**: 2239–2250.

Kulandaivelu, G., and Noorudeen, A.M. (1983) Comparative study of the action of ultraviolet-C and ultraviolet-B on photosynthetic electron transport. *Physiol Plant* **58**: 389–394.

Li, G., and Gao, K. (2013) Cell size-dependent effects of solar UV radiation on primary production in coastal waters of the South China Sea estuaries and coasts. *Estuar Coast* **36**: 728–736.

Li, J., Ou-Lee, T.M., Raba, R., Amundson, R.G., and Last, R.L. (1993) *Arabidopsis* flavonoid mutants are hypersensitive to UV-B irradiation. *Plant Cell* **5**: 171–179.

Li, D.H., Chen, L.Z., Li, G.B., Wang, G.H., Song, L.R., and Liu, Y.D. (2005) Photoregulated or energy dependent process of hormogonia differentiation in *Nostoc sphaeroides* Kützing (cyanobacterium). *J Integr Plant Biol* **47**: 709–716.

Li, G., Che, Z., and Gao, K. (2013) Photosynthetic carbon fixation by tropical coral reef phytoplankton assemblages: a UVR perspective. *Algae* **28**: 281–288.

Lichtenthaler, H.K., and Buschmann, C. (2001) Chlorophylls and carotenoids: measurement and characterization by UV-VIS spectroscopy. In *Current Protocols in Food Analytical Chemistry*, Wrolstad, R.E., Acree, T.E., Decker, E.A., Penner, M.H., Reid, D.S., Schwartz, S.J., *et al*. (eds). New York: Wiley, pp. F431–F438.

Liu, S.W., and Qiu, B.S. (2012) Different responses of photosynthesis and flow cytometric signals to iron limitation and nitrogen source in coastal and oceanic *Synechococcus* strains (Cyanophyceae). *Mar Biol* **159**: 519–532.

McLeod, G.C., and Kanwisher, J. (1962) The quantum efficiency of photosynthesis in the ultraviolet light. *Physiol Plant* **15**: 581–586.

Murakami, A. (1997) Quantitative analysis of 77 K fluorescence emission spectra in *Synechocystis* sp. PCC 6714 and *Chlamydomonas reinhardtii* with variable PSI/PSII stoichiometries. *Photosynth Res* **53**: 141–148.

Murakami, A., and Fujita, Y. (1991) Steady state of photosynthetic electron transport in cells of the cyanophyte *Synechocystis* PCC 6714 having different stoichiometry between PSI and PSII: analysis of flash-induced oxidation-reduction of cytochrome *f* and P700 under steady state of photosynthesis. *Plant Cell Physiol* **32**: 213–222.

Murakami, A., and Fujita, Y. (1993) Regulation of stoichiometry between PSI and PSII in response to light regime for photosynthesis observed with *Synechocystis* PCC 6714: relationship between redox state of Cyt b_6-*f* complex and regulation of PSI formation. *Plant Cell Physiol* **34**: 1175–1180.

Neale, P.J., Bossard, P., Huot, Y., and Sommaruga, R. (2001) Incident and *in situ* irradiance in lakes Cadagno and Lucerne: a comparison of methods and models. *Aquat Sci* **63**: 250–264.

Novis, P.M., Whitehead, D., Gregorich, E.G., Hunt, J.E., Sparrow, A.D., Hopkins, D.W., *et al*. (2007) Annual carbon fixation in terrestrial populations of *Nostoc commune* (cyanobacteria) from an Antarctic dry valley is driven by temperature regime. *Glob Chang Biol* **13**: 1224–1237.

Ohad, I., Raanan, H., Keren, N., Tchernov, D., and Kaplan, A. (2010) Light-induced changes within photosystem II protects *Microcoleus* sp. in biological desert sand crusts against excess light. *PLoS One* **5**: e11000.

Partensky, F., Hess, W.R., and Vaulot, D. (1999) *Prochlorococcus*, a marine photosynthetic prokaryote of global significance. *Microbiol Mol Biol Rev* **63**: 106–127.

Paul, N.D., and Gwynn-Jones, D. (2003) Ecological roles of solar UV radiation: towards an integrated approach. *Trends Ecol Evol* **18**: 48–55.

Poulson, M.E., Donahue, R.A., Konvalinka, J., and Boeger, M.R.T. (2002) Enhanced tolerance of photosynthesis to high-light and drought stress in *Pseudotsuga menziesii* seedlings grown in ultraviolet-B radiation. *Tree Physiol* **22**: 829–838.

Qiu, B.S., Liu, J.Y., Liu, Z.L., and Liu, S.X. (2002) Distribution and ecology of the edible cyanobacterium Ge-Xian-Mi (*Nostoc*) in rice fields of Hefeng County in China. *J Appl Phycol* **14**: 423–429.

Rastogi, R.P., Sinha, R.P., Moh, S.H., Lee, T.K., Kottuparambil, S., Kim, Y.J., *et al*. (2014) Ultraviolet radiation and cyanobacteria. *J Photochem Photobiol B* **141**: 154–169.

Raven, J.A., and Kübler, J.E. (2002) New light on the scaling of metabolic rate with the size of algae. *J Phycol* **38**: 11–16.

Renger, G., Gräber, P., Dohnt, G., Hagemann, R., Weiss, W., and Voss, R. (1982) The effect of UV irradiation on primary

processes of photosynthesis. In *Biological Effects of UV-B Radiation*, Bauer, H., Caldwell, M.M., Tevini, M., and Worrest, R.C. (eds). München: Gesellschaft für Strahlen und Umweltforschung mbH, pp. 110–116.

Rizzini, L., Favory, J.J., Cloix, C., Faggionato, D., O'Hara, A., Kaiserli, E., *et al*. (2011) Perception of UV-B by the *Arabidopsis* UVR8 protein. *Science* **332**: 103–106.

Robson, T.M., Aphalo, P.J., Banaś, A.K., Barnes, P.W., Brelsford, C.C., Jenkins, G.I., *et al*. (2019) A perspective on ecologically relevant plant-UV research and its practical application. *Photochem Photobiol Sci* **18**: 970–988.

Salomon, E., and Keren, N. (2011) Manganese limitation induces changes in the activity and in the organization of photosynthetic complexes in the cyanobacterium *Synechocystis* sp. strain PCC 6803. *Plant Physiol* **155**: 571–579.

Sand-Jensen, K. (2014) Ecophysiology of gelatinous *Nostoc* colonies: unprecedented slow growth and survival in resource-poor and harsh environments. *Ann Bot* **114**: 17–33.

Shang, J.L., Zhang, Z.C., Yin, X.Y., Chen, M., Hao, F.H., Wang, K., *et al*. (2018) UV-B induced biosynthesis of a novel sunscreen compound in solar radiation and desiccation tolerant cyanobacteria. *Environ Microbiol* **20**: 200–221.

Shang, J.L., Chen, M., Hou, S., Li, T., Yang, Y.W., Li, Q., *et al*. (2019) Genomic and transcriptomic insights into the survival of the subaerial cyanobacterium *Nostoc flagelliforme* in arid and exposed habitats. *Environ Microbiol* **21**: 845–863.

Shih, P.M. (2015) Cyanobacterial evolution: fresh insight into ancient questions. *Curr Biol* **25**: R192–R193.

Singh, S.P., Häder, D.P., and Sinha, R.P. (2010) Cyanobacteria and ultraviolet radiation (UVR) stress: mitigation strategies. *Ageing Res Rev* **9**: 79–90.

Smith, R.C., Prézelin, B.B., Baker, K.S., Bidigare, R.R., Boucher, N.P., Coley, T., *et al*. (1992) Ozone depletion: ultraviolet radiation and phytoplankton biology in Antarctic waters. *Science* **255**: 952–959.

Takahashi, S., Milward, S.E., Yamori, W., Evans, J.R., Hillier, W., and Badger, M.R. (2010) The solar action spectrum of photosystem II damage. *Plant Physiol* **153**: 988–993.

Thomas, D.J., Thomas, J., Youderian, P.A., and Herbert, S. K. (2001) Photoinhibition and light-induced cyclic electron transport in *ndhB*- and *psaE*- mutants of *Synechocystis* sp. PCC 6803. *Plant Cell Physiol* **42**: 803–812.

Ungerer, J., Lin, P.C., Chen, H.Y., and Pakrasi, H.B. (2018) Adjustments to photosystem stoichiometry and electron transfer proteins are key to the remarkably fast growth of the cyanobacterium *Synechococcus elongatus* UTEX 2973. *MBio* **9**: e02327–e02317.

Van Liere, L., and Walsby, A.E. (1982) Interactions of cyanobacteria with light. In *The Biology of Cyanobacteria*, Carr, N.G., and Whitton, B.A. (eds). Oxford, UK: Blackwell Sci Publications, pp. 9–45.

Volkmer, T., Schneider, D., Bernát, G., Kirchhoff, H., Wenk, S.O., and Rögner, M. (2007) Ssr2998 of *Synechocystis* sp. PCC 6803 is involved in regulation of cyanobacterial electron transport and associated with the cytochrome b_6f complex. *J Biol Chem* **282**: 3730–3737.

Wargent, J.J., Elfadly, E.M., Moore, J.P., and Paul, N.D. (2011) Increased exposure to UV-B radiation during early development leads to enhanced photoprotection and improved long-term performance in *Lactuca sativa*. *Plant Cell Environ* **34**: 1401–1413.

Wargent, J.J., Nelson, B.C.W., McGhie, T.K., and Barnes, P. W. (2015) Acclimation to UV-B radiation and visible light in *Lactuca sativa* involves up-regulation of photosynthetic performance and orchestration of metabolome-wide responses. *Plant Cell Environ* **38**: 929–940.

Wiethaus, J., Busch, A.W.U., Dammeyer, T., and Frankenberg-Dinkel, N. (2010) Phycobiliproteins in *Prochlorococcus marinus*: biosynthesis of pigments and their assembly into proteins. *Eur J Cell Biol* **89**: 1005–1010.

Williamson, C.E., Neale, P.J., Hylander, S., Rose, K.C., Figueroa, F.L., Robinson, S.A., *et al*. (2019) The interactive effects of stratospheric ozone depletion, UV radiation, and climate change on aquatic ecosystems. *Photochem Photobiol Sci* **18**: 717–746.

Wu, H., Gao, K., Ma, Z., and Watanabe, T. (2005) Effects of solar ultraviolet radiation on biomass production and pigment contents of *Spirulina platensis* in commercial operations under sunny and cloudy weather conditions. *Fisheries Sci* **71**: 454–456.

Wu, H., Abasova, L., Cheregi, O., Deák, Z., Gao, K., and Vass, I. (2011) D1 protein turnover is involved in protection of photosystem II against UV-B induced damage in the cyanobacterium *Arthrospira* (*Spirulina*) *platensis*. *J Photochem Photobiol B* **104**: 320–325.

Xu, J., and Gao, K. (2010) UV-A enhanced growth and UV-B induced positive effects in the recovery of photochemical yield in *Gracilaria lemaneiformis* (Rhodophyta). *J Photochem Photobiol B* **100**: 117–122.

Xu, J., and Gao, K. (2016) Photosynthetic contribution of UV-A to carbon fixation by macroalgae. *Phycologia* **55**: 318–322.

Xu, K., and Qiu, B.S. (2007) Responses of superhigh-yield hybrid rice Liangyoupeijiu to enhancement of ultraviolet-B radiation. *Plant Sci* **172**: 139–149.

Yamori, W., and Shikanai, T. (2016) Physiological functions of cyclic electron transport around photosystem I in sustaining photosynthesis and plant growth. *Annu Rev Plant Biol* **67**: 81–106.

Yang, Y.Q., and Yao, Y. (2008) Photosynthetic responses to solar UV-A and UV-B radiation in low- and high-altitude populations of *Hippophae rhamnoides*. *Photosynthetica* **46**: 307–311.

Yu, L., Zhao, J., Mühlenoff, U., Bryant, D.A., and Golbeck, J. H. (1993) PsaE is required for *in vivo* cyclic electron flow around photosystem I in the cyanobacterium *Synechococcus* sp. PCC 7002. *Plant Physiol* **103**: 171–180.

Zhang, P.Y., Tang, X.X., Cai, H.J., Yu, J., and Yang, Z. (2005) Effects of UV-B radiation on protein and nucleic acid synthesis in three species of marine Red-Tide microalgae. *Acta Phytoecol Sin* **29**: 505–509. (in Chinese)

Supporting Information

Additional Supporting Information may be found in the online version of this article at the publisher's web-site:

Fig. S1 Effects of UV-A radiation from the UV-B lamp on growth of *N. sphaeroides*. (A) Energy emission spectrum of

UV-A from the UV-B lamp (0.33 W m^{-2}) filtered by a Folex 320 (Montagefolieno, no. 10155099; Folex, Dreieich, Germany) plus ultra white glass filter (Supporting Information Fig. S2B). (B) Growth curve based on chlorophyll *a* (Chl *a*) content during 14 d exposure to photosynthetically active radiation (PAR) or PAR plus UV-A. (C) Dry weight measured after 14 d exposure to UV-A. Bars with different superscript letters are significantly different (*t*-test, $P < 0.05$). Data are means $\pm$ S.D. ($n = 5–6$).

Fig. S2. Energy emission spectrum of the UV-B lamp (A), transmission spectrum of the ultra white glass filter (B), and weighted UV radiation (C) based on the biological spectral weighted function of Flint and Caldwell (2003) for UV-B treated samples.

Table S1. Realistic levels of UV-B radiation and their typical effects on various photosynthetic organisms reported in the literature.

Appendix S1: Supporting Information